Proc. Natl. Acad. Sci. USA
Vol. 93, pp. 6981–6985, July 1996
Biochemistry

Binding site size limit of the 2:1 pyrrole-imidazole polyamide-DNA motif

JAMES J. KELLY, ELDON E. BAIRD, AND PETER B. DERVAN*

Division of Chemistry and Chemical Engineering, California Institute of Technology, Pasadena, CA 91125

Contributed by Peter B. Dervan, March 26, 1996

ABSTRACT **Polyamides containing *N*-methylimidazole (Im) and *N*-methylpyrrole (Py) amino acids can be combined in antiparallel side-by-side dimeric complexes for sequence-specific recognition in the minor groove of DNA. Six polyamides containing three to eight rings bind DNA sites 5–10 bp in length, respectively. Quantitative DNase I footprint titration experiments demonstrate that affinity maximizes and is similar at ring sizes of five, six, and seven. Sequence specificity decreases as the length of the polyamides increases beyond five rings. These results provide useful guidelines for the design of new polyamides that bind longer DNA sites with enhanced affinity and specificity.**

Recent examples of 2:1 polyamide-DNA complexes have created new models for the design of nonnatural ligands for specific recognition of a broad sequence repertoire in the minor groove of DNA (1–13). The side-by-side combination of one imidazole ring on one ligand and a pyrrolecarboxamide on the second ligand is specific for G·C, whereas a pyrrolecarboxamide/imidazole pair targets a C·G base pair (1–3). A pyrrolecarboxamide/pyrrolecarboxamide pair is partially degenerate and binds A·T or T·A base pairs (4–6). The DNA sequence specificities of these small molecules can be controlled by the linear sequences of pyrrole and imidazole amino acids. The three-ring polyamide Im-(Py)$_2$-Dp (consisting of *N*-methylimidazole, *N*-methylpyrrole, and *N*,*N*-dimethylaminopropylamide, respectively) was shown to specifically bind 5-bp 5′-(A,T)G(A,T)C(A,T)-3′ sequences (1–3), whereas the four-ring polyamide ImPyImPy-Dp was shown to bind 6-bp 5′-(A,T)GCGC(A,T)-3′ sites (10, 11) as side-by-side antiparallel dimers in the minor groove.

A major goal of our efforts in evaluating the scope and limitations of the 2:1 polyamide-DNA motif is to extend specific recognition to larger binding sites. To determine the effect of polyamide length on binding site size, binding affinity, and sequence specificity within the motif, a series of six pyrroleimidazole polyamides containing three to eight rings was synthesized. The polyamide series is based on Im-(Py)$_2$-Dp (Fig. 1, **1**) with pyrrolecarboxamide moieties added sequentially to the C termini to afford Im-(Py)$_3$-Dp (**2**), Im-(Py)$_4$-Dp (**3**), Im-(Py)$_5$-Dp (**4**), Im-(Py)$_6$-Dp (**5**), and Im-(Py)$_7$-Dp (**6**), which are designed to bind 5- to 10-bp sites, respectively, as side-by-side antiparallel dimers (Fig. 2). The DNA binding sites are based on a 5′-TGACA-3′ core sequence and contain sequential A,T base pair inserts in the center of the binding sites that will be recognized by the additional pyrrolecarboxamides. This combination of polyamides and DNA binding site sequences was chosen to satisfy several criteria. The presence of G·C and C·G base pairs in the binding sites is expected to lock the polyamides in the designated binding sites by preventing them from binding in undesired slipped conformations on the DNA (13). The alternating A,T tract in the center of the binding sites is designed to favor 2:1 binding in contrast to pure A tracts, which generally favor 1:1 polyamide-DNA complex formation (14, 15). The binding site size was determined by MPE·Fe(II) footprinting (16), and the apparent first order binding affinity and sequence specificity of each polyamide was determined by quantitative DNase I footprint titration experiments (17) on a series of restriction fragments containing a match site and a single base pair mismatch site for each polyamide.

MATERIALS AND METHODS

NMR spectra were recorded on a GE 300 instrument operating at 300 MHz. Spectra were recorded in dimethyl sulfoxide d_6 (DMSO-d_6) with chemical shifts reported in parts per million relative to residual DMSO-d_5. High resolution fast atom bombardment (FAB) mass spectra were recorded at the Mass Spectroscopy Laboratory at the University of California, Riverside. Matrix-assisted, laser desorption/ionization time of flight mass spectrometry was carried out at the Protein and Peptide Microanalytical Facility at the California Institute of Technology. Preparative HPLC was carried out on a Beckman instrument using a Waters DeltaPak 25 × 100 mm, 100-μm C_{18} column in 0.1% (wt/vol) trifluoroacetic acid (TFA), gradient elution 0.25%/min CH_3CN.

Aminohexa-(*N*-methylpyrrolecarboxamide) ditrifluoroacetate 7. To a solution of *N*-(*tert*-butoxycarbonyl)-tris(*N*-methylpyrrolecarboxamide) (20 mg, 41 μmol) in *N*,*N*-dimethylformamide (100 μl) was added 2-(1H-Benzotriazole-1-yl)-1,1,3,3-tetramethyluronium hexafluorophosphate (HBTU) (26 mg, 69 μmol) followed by *N*,*N*-diisopropylethylamine (DIEA) (50 μl, 288 μmol). The reaction was allowed to stand for 5 min, agitated, and allowed to stand for an additional 5 min. Aminotris-(*N*-methylpyrrolecarboxamide) (24 mg, 41 μmol) was then added, followed by DIEA (50 μl, 288 μmol), and the reaction was agitated for 2 hr. The reaction mixture was concentrated *in vacuo*, and TFA (10 ml) was added. After 2 min, the TFA was removed *in vacuo*. Purification of the resulting brown oil by reversed phase HPLC afforded the diamine **7** (see Fig. 3) as a white powder. Yield: 26 mg (58%); ^{1}H NMR (DMSO-d_6) δ 10.06 (s, 1 H), 9.95 (m, 2 H), 9.91 (s, 1 H), 9.84 (s, 1 H), 9.44 (br s, 1 H), 8.16 (t, 1 H, J = 4.0 Hz), 7.22 (m, 4 H), 7.16 (d, 1 H, J = 1.7 Hz), 7.10 (s, 1 H, J = 1.7 Hz), 7.07 (m, 3 H), 6.98 (s, 1 H, J = 1.7 Hz), 6.93 (s, 1 H, J = 1.8 Hz), 3.88 (m, 6 H), 3.84 (m, 12 H), 3.79 (m, 6 H), 3.21 (m, 2 H), 3.04 (m, 2 H), 2.77 (d, 6 H, J = 4.8 Hz), 1.80 (m, 2 H); FABMS m/e 835.412 (M + H, 835.416 calculated for $C_{41}H_{51}N_{14}O_6$).

Im(Py)$_6$-Dp 5. *N*-methylimidazole-2-carboxylic acid (100 mg, 741 μmol) and hydroxybenzotriazole (72 mg, 500 μmol) were suspended in 500 μl *N*,*N*-dimethylformamide. Upon addition of dicyclohexylcarbodiimide (100 mg, 500 μmol), the

Abbreviations: Im, *N*-methylimidazole; Py, *N*-methylpyrrole; Dp, *N*,*N*-dimethylaminopropylamide; DMSO, dimethyl sulfoxide; FAB, fast atom bombardment; TFA, trifluoroacetic acid; HBTU, 2-(1H-benzotriazole-1-yl)-1,1,3,3-tetramethyluronium hexafluorophosphate; DIEA, *N*,*N*-diisopropylethylamine.

*To whom reprint requests should be addressed.

The publication costs of this article were defrayed in part by page charge payment. This article must therefore be hereby marked "*advertisement*" in accordance with 18 U.S.C. §1734 solely to indicate this fact.

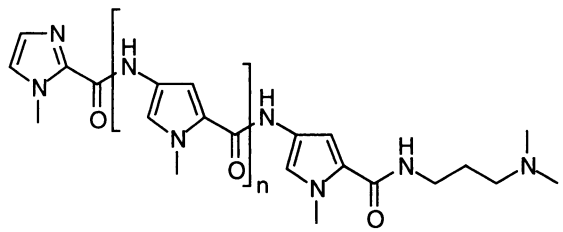

Im-$(Py)_2$-Dp, **1**, n = 1
Im-$(Py)_3$-Dp, **2**, n = 2
Im-$(Py)_4$-Dp, **3**, n = 3
Im-$(Py)_5$-Dp, **4**, n = 4
Im-$(Py)_6$-Dp, **5**, n = 5
Im-$(Py)_7$-Dp, **6**, n = 6

FIG. 1. Structures of the pyrroleimidazole polyamides Im-$(Py)_2$-Dp, Im-$(Py)_3$-Dp, Im-$(Py)_4$-Dp, Im-$(Py)_5$-Dp, Im-$(Py)_6$-Dp, and Im-$(Py)_7$-Dp.

reaction mixture became a homogeneous solution. The activation was allowed to stand for 12 hr, precipitated dicyclohexylurea was removed by filtration, and **7** (10 mg, 9.4 μmol) was added followed by DIEA (100 μl, 576 μmol); the reaction was allowed to stand for 2 hr. Reversed phase HPLC purification of the reaction mixture afforded **5** as a white powder. Yield: 6.3 mg (62%); HPLC, r.t. 27.4 min; UV (H_2O) λ_{max} (ε), 246 (34, 100), 304 (56, 600) nm; ^1H NMR (DMSO-d_6) δ 10.46 (s, 1 H), 9.55 (s, 1 H), 9.94 (m, 3 H), 9.90 (s, 1 H), 9.20 (br s, 1 H), 8,14 (t, 1 H, J = 7.2 Hz), 7.38 (s, 1 H), 7.28 (d, 1 H, J = 1.4 Hz), 7.26 (d, 1 H, J = 1.4 Hz), 7.23 (m, 4 H), 7.08 (m, 5 H), 7.04 (s, 1 H, J = 1.2 Hz), 6.93 (d, 1 H, J = 1.6 Hz), 3.98 (s, 3 H), 3.84 (m, 15 H), 3.83 (s, 1 H), 3.30 (q, 2 H, J = 7.4 Hz), 3.21 (t, 2 H, J = 7.1 Hz), 2.77 (d, 6 H, J = 4.1 Hz), 1.74 (m, 2 H); MALDI-TOF MS 944.21 (M + H 944.04 calculated); FABMS *m/e* 965.430 (M + Na, 965.426 calculated for $C_{46}H_{54}N_{16}O_7Na$).

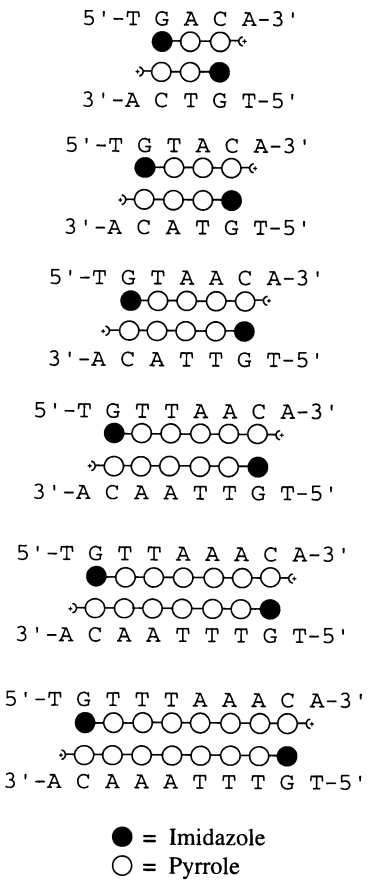

FIG. 2. Proposed 2:1 binding models of Im-$(Py)_2$-Dp, Im-$(Py)_3$-Dp, Im-$(Py)_4$-Dp, Im-$(Py)_5$-Dp, Im-$(Py)_6$-Dp, and Im-$(Py)_7$-Dp binding to 5-, 6-, 7-, 8-, 9-, and 10-bp match sites, respectively. The imidazole and pyrrole rings are represented as shaded and unshaded spheres, respectively.

DNA Manipulations. Plasmids pJK5, pJK6, pJK7, pJK8, pJK9, and pJK10 were prepared by ligation of oligonucleotide duplexes containing the desired insert sequences into *Bam*HI/*Hin*dIII-restricted pUC19 DNA using Epicurean Coli XL1-Blue Supercompetent cells (Stratagene) according to the manufacturer's protocol. Plasmids were isolated using a Qiagen (Chatsworth, CA) maxiprep kit (Tip 500), and the sequences were confirmed by dideoxy sequencing. General manipulations of DNA were performed according to established procedures (18). MPE·Fe(II) footprint experiments and Quantitative DNase I footprint titration experiments were carried out as previously described (1, 12).

RESULTS AND DISCUSSION

Polyamide Synthesis. Im-$(Py)_2$-Dp was prepared as previously described (6). Polyamides **2–6** were prepared in two steps from previously described intermediates exemplified for Im-$(Py)_6$-Dp **5**; full synthetic details will be described elsewhere (Fig. 3). Activation of *N*-(*tert*-butoxycarbonyl)-tris(*N*-methylpyrrole-carboxamide) (19) with HBTU followed by coupling to aminotris(*N*-methylpyrrolecarboxamide) (12) provided *N*-(*tert*-butoxycarbonyl)-hexa(*N*-methylpyrrolecarboxamide). The amine was deprotected by the addition of neat TFA to the crude reaction mixture, and the ditrifluoroacetate salt of aminohexa(*N*-methylpyrrolecarboxamide) was isolated by preparatory HPLC. Capping with 1-methylimidazole-2-carboxylic acid (1) (dicyclohexylcarbodiimide/hydroxybenzotriazole) provided Im-$(Py)_6$-Dp **5** after HPLC purification.

Binding Site Sizes. Binding site sizes were determined by MPE·Fe(II) footprinting of **1–6** on six restriction fragments from plasmids pJK5 through pJK10, respectively (Fig. 4). Each restriction fragment contains a match and a single base pair mismatch site separated by 10 bp. The single base pair mismatch is generated by a G·C base pair replacing an A·T or T·A base pair in the center of the binding site. Analysis of the MPE·Fe(II) protection patterns reveals that the sequential addition of pyrrolecarboxamide moieties to the C termini of the polyamides increases the preferred DNA binding site size by 1 bp (Fig. 5). For all six polyamides, the observed MPE·Fe(II) protection patterns are 3′-shifted, consistent with 2:1 polyamide-DNA complex formation in the minor groove.

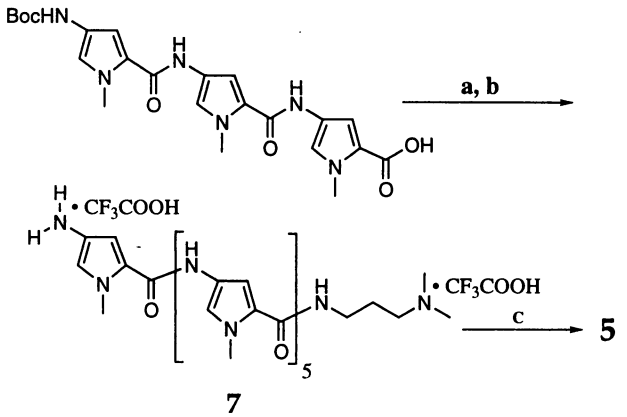

FIG. 3. Synthesis of ImPyPyPyPyPyPy-Dp. (*a*) (*i*) HBTU, DIEA; (*ii*) aminotris(1-methylpyrrole-2-carboxamide), DIEA. (*b*) TFA. (*c*) 1-methylimidazole-2-carboxylic acid, hydroxybenzotriazole, dicyclohexylcarbodiimide, DIEA.

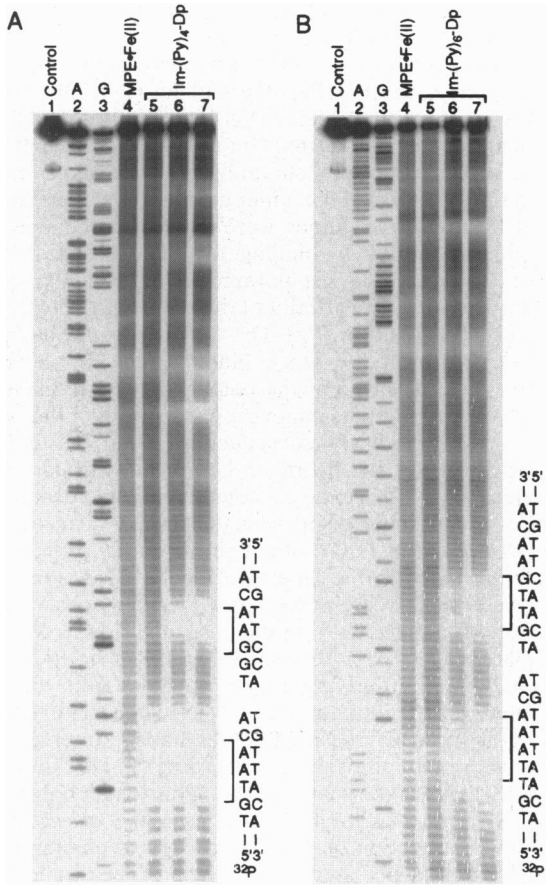

FIG. 4. MPE·Fe(II) footprinting experiments of Im-$(Py)_4$-Dp (*A*) and Im-$(Py)_6$-Dp (*B*) on the *Eco*RI/*Pvu*II restriction fragments from plasmids pJK7 and pJK10, respectively. Gray scale representations of storage phosphor autoradiograms of 8% denaturing polyacrylamide gels. All reactions contain 25 mM Tris·AcOH (pH 7.0), 10 mM NaCl, 100 μM bp calf thymus DNA, 5 μM MPE·Fe(II), 5 mM DTT, and 20–30 kcpm of 3′-^{32}P-labeled restriction fragment. Lanes 1–4 in *A* and *B* correspond to intact DNA, A reaction, G reaction, and a MPE·Fe(II) control to which no polyamide was added, respectively. Lanes 5–7 correspond to 2, 5, and 10 μM Im-$(Py)_4$-Dp (*A*) and Im-$(Py)_6$-Dp (*B*), respectively. Brackets indicate the approximate location of the match and mismatch sites.

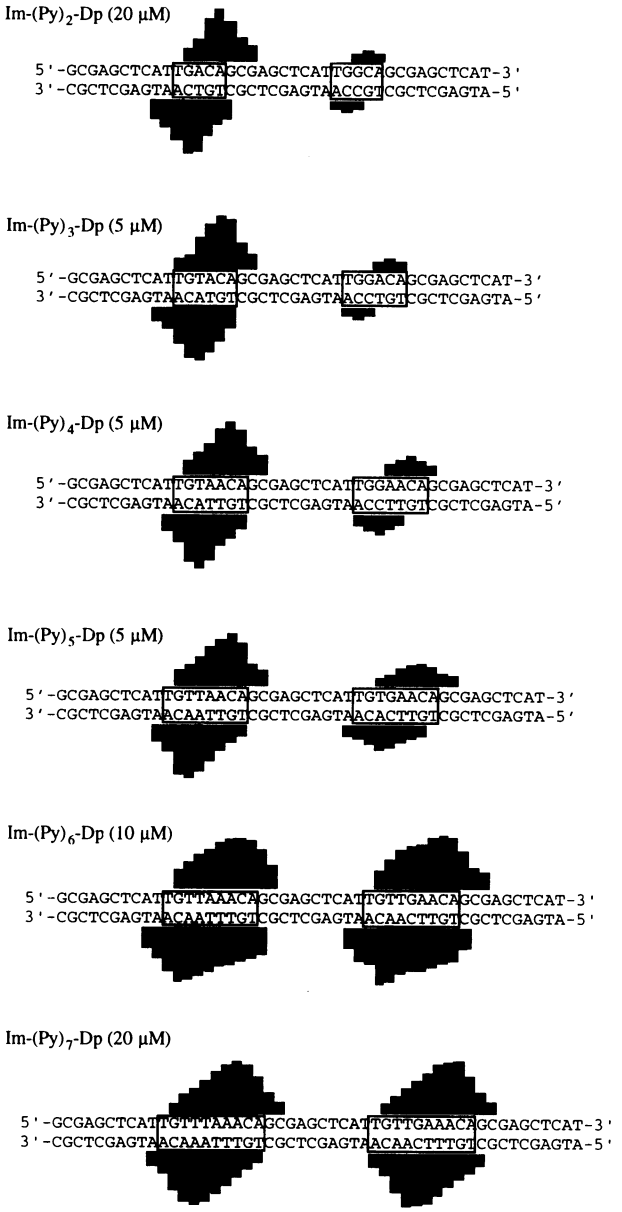

FIG. 5. Histograms of cleavage protection from MPE·Fe(II) for Im-$(Py)_2$-Dp, Im-$(Py)_3$-Dp, Im-$(Py)_4$-Dp, Im-$(Py)_5$-Dp, Im-$(Py)_6$-Dp, and Im-$(Py)_7$-Dp binding to the *Eco*RI/*Pvu*II restriction fragments from plasmids pJK5, pJK6, pJK7, pJK8, pJK9, and pJK10, respectively. The individual bar heights are proportional to the protection from MPE·Fe(II) cleavage at each nucleotide. The match and mismatch sites are indicated by boxes.

Affinities. The equilibrium association constants for the match and single base pair mismatch sites for the six polyamides were determined by quantitative DNase I footprint titration experiments (10 mM Tris·HCl, pH 7.0/10 mM KCl/5 mM $MgCl_2$/5 mM $CaCl_2$; 22°C) in the absence of unlabeled carrier DNA. The θ_{app} points for each polyamide were steep and adequately fit by a cooperative binding isotherm, consistent with 2:1 polyamide-DNA complex formation (Fig. 6) (11). Analysis of the match site data reveals that Im-$(Py)_2$-Dp binds the 5-bp 5′-TGACA-3′ site with an equilibrium association constant, K_a of 1.3×10^5 M^{-1}, whereas Im-$(Py)_3$-Dp binds the 6-bp 5′-TGTACA-3′ site with $K_a = 8.6 \times 10^6$ M^{-1}, corresponding to a 66-fold enhancement in affinity (Table 1). The five-ring polyamide Im-$(Py)_4$-Dp binds the seven-bp site 5′-TGTAACA-3′ with $K_a = 4.5 \times 10^7$ M^{-1}, a 5-fold gain in affinity. Binding affinity levels off with Im-$(Py)_5$-Dp binding the 8-bp 5′-TGTTAACA-3′ site ($K_a = 5.3 \times 10^7$ M^{-1}) and Im-$(Py)_6$-Dp binding the 9-bp 5′-TGTTAAACA-3′ site ($K_a = 4.7 \times 10^7$ M^{-1}) with the same affinity as Im-$(Py)_4$-Dp for a 7-bp site. Binding affinity drops dramatically for Im-$(Py)_7$-Dp binding to a 10-bp 5′-TGTTTAAACA-3′ site ($K_a < 2 \times 10^6$ M^{-1}).

The 66-fold enhancement in affinity for Im-$(Py)_3$-Dp binding to a 6-bp 5′-TGTACA-3′ site compared with Im-$(Py)_2$-Dp binding to a 5-bp 5′-TGACA-3′ site corresponds to an increase in the free energy of binding ($\Delta\Delta G$) of 2.4 kcal/mol (22°C). This increase in the free energy of binding is likely a result of the additional pyrrolecarboxamide/pyrrolecarboxamide pair in the Im-$(Py)_3$-Dp dimer recognizing the T·A base pair in the context of the 5′-TGTACA-3′ sequence. A significant fraction of the increase in binding affinity for Im-$(Py)_3$-Dp presumably results from the hydrogen bonds and van der Waals contacts that likely form when the additional pyrrolecarboxamides in the ligand bind the additional T·A base pair in the core of the binding site. The 5-fold enhancement in affinity of Im-$(Py)_4$-Dp for the 7-bp 5′-TGTAACA-3′ site over Im-$(Py)_3$-Dp binding to 5′-TGTACA-3′ corresponds to an increase in the free energy of binding of 1.0 kcal/mol. This relatively modest change in binding free energy suggests that the addition of a pyrrolecarboxamide moiety to the four-ring Im-$(Py)_3$-Dp is less favorable. The observation that the affinities of Im-

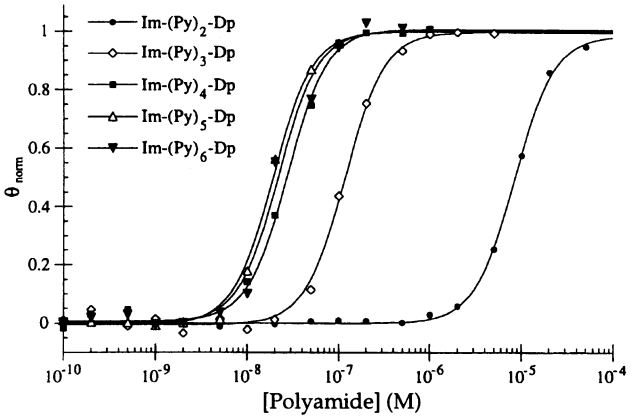

FIG. 6. Data for the quantitative DNase I footprint titration experiments for Im-$(Py)_{2-6}$-Dp in complex with the 5- to 9-bp match sites. The curve through each set of data points is the best-fit cooperative Langmuir binding titration isotherm (n = 2) obtained from a nonlinear least-squares algorithm.

$(Py)_5$-Dp and Im-$(Py)_6$-Dp for the 8- and 9-bp 5′-TGTTAACA-3′ and 5′-TGTTAAACA-3′ sites, respectively, are the same as Im-$(Py)_4$-Dp binding 5′-TGTAACA-3′ indicates that further lengthening of the polyamides from five to seven rings and the DNA binding site from 7 to 9 bp has little energetic benefit. The dramatic decrease in affinity of Im-$(Py)_7$-Dp for the 10-bp 5′-TGTTTAAACA-3′ site ($K_a < 2 \times 10^6$ M^{-1}) suggests that the presence of an additional pyrrolecarboxamide in the ligand creates an unfavorable contribution to the binding free energy of Im-$(Py)_7$-Dp for the 5′-TGTTTAAACA-3′ site.

Specificities. Comparison of the equilibrium association constants for the match and the single base pair mismatch site for each polyamide demonstrates that the specificity of 2:1 polyamide-DNA complex formation, defined as the ratio of match site binding affinity to the affinity for the single base pair mismatch site, generally decreases with increasing polyamide length as the polyamide length increases beyond five rings (Table 1). Im-$(Py)_2$-Dp prefers binding the 5′-TGACA-3′ site over the 5′-TGGCA-3′ site by a factor of at least 6.5. Im-$(Py)_3$-Dp and Im-$(Py)_4$-Dp bind the mismatch sites with 5- and 6-fold lower affinity, respectively. Im-$(Py)_5$-Dp displays at least a 3-fold preference for the match site, whereas Im-$(Py)_6$-Dp binds the mismatch site with 2.7-fold lower affinity. At concentrations below 1 μM, Im-$(Py)_7$-Dp shows no binding to DNA. At concentrations of 1 μM and above, equal protection from cleavage by DNase I of both the match and mismatch sites is observed, indicating that the specificity as defined here is approximately 1 (data not shown).

One explanation for these observations is that the three- and four-ring polyamides Im-$(Py)_2$-Dp and Im-$(Py)_3$-Dp, respectively, are in phase with their DNA binding sites. NMR and molecular modeling of a related (Im-$(Py)_2$-Dp)$_2$·5′-TGACT-3′ complex showed that the curvature of the ligand closely matched the curvature of the minor groove of the 5-bp binding site (2). Similar observations were made for the four-ring polyamide ImPyImPy-Dp binding to a 5′-AGCGCT-3′ sequence (10). For the longer polyamides beginning with Im-$(Py)_4$-Dp, where binding affinities level off at Im-$(Py)_5$-Dp and ultimately decrease at Im-$(Py)_7$-Dp, the ligands may be falling out of register with the DNA binding sites. In these 2:1 complexes, the curvature of the polyamides would likely not match the curvature of the minor groove surfaces of the longer binding sites. One likely consequence would be that the energetic benefit of the hydrogen bonds and van der Waals interactions that stabilize the 2:1 complexes would decrease as the lack of correspondence between the binding surfaces of the polyamides and the DNA sites became more pronounced. Register mismatch in the larger polyamide-DNA complexes may explain the decrease in sequence specificity observed for the longer polyamides. (15). In the mismatch sites, a G·C base pair replaces an A·T or T·A base pair in the core of the binding site. The 2-amino group of guanine protrudes from the floor of the minor groove and, therefore, is expected to introduce a bump on the surface of the binding sites that may interfere with the hydrogen bonding of the pyrrolecarboxamide NH of the polyamides to N3 of the guanine base. If the longer polyamides are out of register with the DNA, then the effect of this unfavorable interaction on the free energy of binding at the mismatch site may become less significant. This would lower the overall free energy difference between binding the match and mismatch sites and thereby reduce specificity.

Sequence-dependent DNA structural features, such as intrinsic minor groove width, minor groove flexibility, and inherent curvature, may differ between each of the binding sites and could contribute to the measured difference in the binding affinities of the six polyamides (14). One possibility is that as the length of the A,T tract in the binding sites increases, the minor groove width and/or flexibility may decrease, which would likely impose an energetic penalty for 2:1 polyamide-DNA complex formation and lower the apparent affinities for these sites. These effects may also contribute to the lower sequence specificity observed for the longer polyamides in the series. Insertion of G·C base pairs into an A·T tract may increase the minor groove width and/or flexibility, which may reduce the difference in binding free energy between the match and mismatch sites, thereby lowering specificity (14).

Table 1. Equilibrium association constants (M^{-1})*†

Polyamide	Rings	Binding site size, bp	Match	Mismatch	Specificity‡
Im-$(Py)_2$-Dp	3	5	1.3×10^5 (0.3)	$<2 \times 10^4$§	>6.5¶
Im-$(Py)_3$-Dp	4	6	8.5×10^6 (1.3)	1.6×10^6 (0.2)	5.3 (0.5)
Im-$(Py)_4$-Dp	5	7	4.5×10^7 (1.1)	7.9×10^6 (1.8)	5.7 (0.8)
Im-$(Py)_5$-Dp	6	8	5.3×10^7 (0.5)	$<2 \times 10^7$§	>2.7¶
Im-$(Py)_6$-Dp	7	9	4.7×10^7 (0.4)	1.7×10^7 (0.7)	2.8 (0.7)
Im-$(Py)_7$-Dp	8	10	$<2 \times 10^6$	$<2 \times 10^6$§	≈1

*Values reported are the mean values from at least three footprint titration experiments. Numbers in parentheses indicate the standard deviation for each data set.

†The assays were performed at 22°C, pH 7.0, in the presence of 10 mM Tris·HCl, 10 mM KCl, 10 mM $MgCl_2$, and 5 mM $CaCl_2$.

‡Defined as the ratio of the match site affinity to the affinity of the single base pair mismatch site. Numbers in parentheses indicate the uncertainty calculated using the standard deviations of the measured binding affinities (19).

§Represents an upper limit for the binding affinity.

¶Represents a lower limit on the specificity.

These considerations of sequence-dependent DNA structure suggest that the sequence composition of the DNA target site may be an important factor in determining polyamide affinity and specificity in the 2:1 motif.

Implications for Design. The results of this study demonstrate that DNA sequences up to 9 bp long can be specifically recognized by pyrroleimidazole polyamides containing three to seven rings by 2:1 polyamide-DNA complex formation in the minor groove. Recognition of a 9-bp site defines the new lower limit of the binding site size that can be recognized by polyamides containing exclusively imidazole and pyrrolecarboxamides. The binding affinity reaches a maximum value for the five-ring polyamide Im-$(Py)_4$-Dp, and addition of up to two additional pyrrolecarboxamides has no effect on the observed binding affinity. These results and the failure of an eight-ring polyamide to specifically recognize a 10-bp site suggests that a new class of polyamides is needed for extension of the 2:1 polyamide-DNA motif to sequences longer than 9 bp. Replacement of a central pyrrole or imidazole amino acid with a more flexible spacer amino acid subunit should allow the antiparallel dimer to reset the register for continued gain in affinity and specificity (20).

We are grateful to the National Institutes of Health for grant support (GM-27681) and a National Research Service Award to J.J.K., and to the Howard Hughes Medical Institute for a predoctoral fellowship to E.E.B.

1. Wade, W. S., Mrksich, M. & Dervan, P. B. (1992) *J. Am. Chem. Soc.* **114,** 8783–8794.
2. Mrksich, M., Wade, W. S., Dwyer, T. J., Geierstanger, B. H., Wemmer, D. E. & Dervan, P. B. (1992) *Proc. Natl. Acad. Sci. USA* **89,** 7586–7590.
3. Wade, W. S., Mrksich, M. & Dervan, P. B. (1993) *Biochemistry* **32,** 11385–11389.
4. Pelton, J. G. & Wemmer, D. E. (1989) *Proc. Natl. Acad. Sci. USA* **86,** 5723–5727.
5. Pelton, J. G. & Wemmer, D. E. (1990) *J. Am. Chem. Soc.* **112,** 1393–1399.
6. Chen, X., Ramakrishnan, B., Rao, S. T. & Sundaralingam, M. (1994) *Struct. Biol. Nat.* **1,** 169–175.
7. Mrksich, M. & Dervan, P. B. (1993) *J. Am. Chem. Soc.* **115,** 2572–2576.
8. Geierstanger, B. H., Jacobsen, J.-P., Mrksich, M., Dervan, P. B. & Wemmer, D. E. (1994) *Biochemistry* **33,** 3055–3062.
9. Geierstanger, B. H., Dwyer, T. J., Bathini, Y., Lown, J. W. & Wemmer, D. E. (1993) *J. Am. Chem. Soc.* **115,** 4474–4482.
10. Geierstanger, B. H., Mrksich, M., Dervan, P B. & Wemmer, D. E. (1994) *Science* **266,** 646–650.
11. Mrksich, M. & Dervan, P. B. (1995) *J. Am. Chem. Soc.* **117,** 3325–3332.
12. Mrksich, M., Parks, M. E. & Dervan, P. B. (1995) *J. Am. Chem. Soc.* **116,** 7983–7988.
13. Geierstanger, B. H., Mrksich, M., Dervan, P. B. & Wemmer, D. E. (1996) *Nat. Struct. Biol.*, **3,** 321–324.
14. Schultz, P. G. & Dervan, P. B. (1983) *Proc. Natl. Acad. Sci. USA* **80,** 6834–6837.
15. Youngquist, R. S. & Dervan, P. B. (1985) *Proc. Natl. Acad. Sci. USA* **82,** 2565–2569.
16. Van Dyke, M. M. & Dervan, P. B. (1984) *Science* **225,** 1122–1127.
17. Brenowitz, M., Senear, D. F., Shea, M. A. & Ackers, G. K. (1986) *Biochemistry* **83,** 8462–8466.
18. Sambrook, J., Fritsch, E. F. & Maniatis, T. (1989) *Molecular Cloning: A Laboratory Manual* (Cold Spring Harbor Lab. Press, Plainview, NY), 2nd Ed.
19. Baily, C., Pommery, N., Houssin, R. & Henichart, J. P. (1989) *J. Pharm. Sci.* **78,** 910–917.
20. Trauger, J. W., Baird, E. E., Mrksich, M. & Dervan, P. B. (1996) *J. Am. Chem. Soc.*, in press.